

The Interconnection between Efficiency and Morphology of two component Systems in Plastic Solar Cells

Franz Padinger, Desta Gebeyehu, Christoph J. Brabec, Thomas Fromherz, and N. Serdar Sariciftci

Christian Doppler Laboratory for Plastic Solar Cells, Johannes Kepler University Linz, A-4040 Austria

Tel.: +43 732 2468 766, Fax: +43 732 2468 770

Email : christoph.brabec@jk.uni-linz.ac.at

Jan C. Hummelen

Stratingh Institute and Materials Science Center, University of Groningen, Nijenborgh 4, 9747 AG Groningen The Netherlands

ABSTRACT

Using the ultrafast photoinduced electron transfer with long-living charge separation in the conjugated polymer/fullerene thin films, photovoltaic devices have been fabricated. The photoinduced charge separation happens with internal quantum efficiency near unity. The performance of such "bulk heterojunction" photovoltaic devices is critically dependent on the transport properties of the interpenetrating network. The influence of the variation of different donor / acceptor materials on the sample morphology is monitored by atomic force microscopy (AFM), while I/V characteristics have been studied to evaluate the conversion efficiency.

INTRODUCTION

The technological advantages for the fabrication of polymer based organic solar cells, like roll to roll production of large areas, may lead to a possible reduction of the production costs. The mechanical flexibility as well as the tunability of the bandgap offer interesting perspectives of polymer based solar cells as compared to solar cells based on inorganic materials. Because of these advantages, the development of polymer solar cells would have a major impact, even if the efficiencies of these types of photovoltaic devices up to now are smaller than the efficiencies achieved in inorganic solar cells.

Conjugated polymers such as derivatives of poly(*para*-phenylenevinylenes), or polythiophenes exhibit an ultrafast photoinduced electron transfer to C₆₀ with forward transfer faster than 200 femtoseconds in the solid state [1, 2]. Thus, the quantum yield of the charge separation in such D/A blends is near unity. The charge separated state, however, is metastable at low temperatures. This photophysical process, resembling the primary steps of photosynthesis, has been utilized to fabricate solar cells [3, 4, 5]. Studies of conjugated polymer/fullerene photovoltaic devices showed that the energy conversion efficiency is limited by the collection of the charges at the electrodes [6].

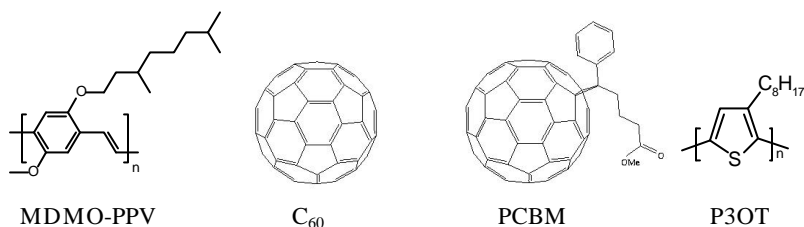


Figure 1: Chemical structure of MDMO-PPV, C_{60} , PCBM and P3OT.

While the excellent photovoltaic response of alkoxy-PPVs with different fullerene-based acceptors has been shown, the class of substituted polythiophenes is known to show a higher tendency of phase separation with fullerenes [7]. It is therefore interesting, to compare these two different classes of conjugated polymers with respect to their photovoltaic behavior in composites with fullerenes. The influence of the different acceptors on the morphology of the interpenetrating network is investigated separately for various substituted fullerenes.

EXPERIMENTAL

The active area of the devices investigated was 4 times 4 cm² on substrates with 6 cm by 6 cm. First the PEDOT-PSS (poly(3,4-ethylenedioxythiophene)-poly(styrenesulfonate) (Baytron – Bayer AG) was spin coated (thickness approximately 100 nm) on transparent ITO (indium tin oxide) -coated polyester substrates (surface resistance of 55 ohm/square). P3OT cells were prepared by spin coating from ~1 wt.% xylene solutions on the top of PEDOT-PSS layer. Photovoltaic devices containing MDMO-PPV as electron donor were produced by doctorblading ~ 0.3% toluene solutions on top of PEDOT. The enhanced solubility of PCBM [8] compared to C_{60} allows a high fullerene / conjugated polymer ratio in donor - acceptor bulk heterojunctions. After an additional drying step the aluminum top electrode was deposited by vacuum evaporation. The thickness of the polymer/fullerene layers was typically in the range of 150 nm.

All cells were produced under ambient room conditions. No actions were taken to remove possibly adsorbed oxygen from the cells. A defocused Ar⁺ laser beam at 488 nm

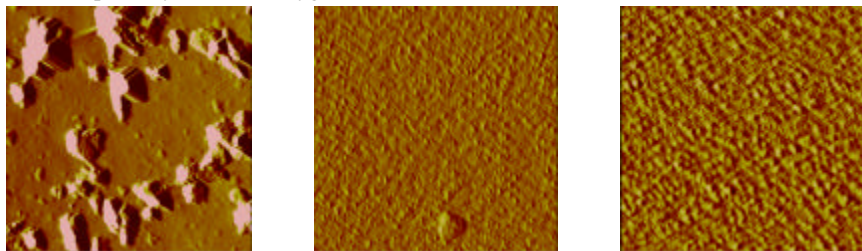


Figure 2: AFM pictures of MDMO-PPV / C_{60} (1:2 wt. ratio – left picture, 50 nm by 50 nm scale), MDMO-PPV / PCBM multiadduct (1:3 wt. ratio – middle picture, 10 nm by 10 nm scale) MDMO-PPV / PCBM monoadduct (1:3 wt. ratio – right picture, 10 nm by 10 nm scale).

provided monochromatic illumination. Light intensities were measured by a calibrated Si Photodiode. A Keithley SMU 2400 Source Meter was used to record the I/V curves by illuminating the cells through the ITO side, typically by averaging 80 - 200 measurements for one point. White light measurements were performed with excitation of 6 mW/cm^2 from a luminescence tube.

Generally, AFM pictures were taken directly from the devices after the I/V measurements.

RESULTS AND DISCUSSION

Figure 2 shows AFM pictures of solar cells made from solutions of MDMO-PPV with PCBM monoadduct (right), PCBM multiadduct (middle) and C_{60} (left). The most homogenous surface is observed for the MDMO-PPV / PCBM multiadduct device. Contrary to the single isomer PCBM monoadduct, the multiadduct consists of a mixture of many isomers of mainly bos-methanofullerenes, ensuring high solubility and miscibility compared to C_{60} or PCBM monoadduct. PCBM monoadduct again gives a rather homogeneous film surface, however, not as smooth as with PCBM multiadduct. This increasing roughness for MDMO-PPV / PCBM monoadduct might be related to the higher tendency of the monoadduct to crystallize compared to the multiadduct. In the case of MDMO-PPV / C_{60} particles on a μm scale can be observed. As all solutions were filtered by $0.2 \mu\text{m}$ syringe filters before casting, these large particles must have formed during the drying process of the films and are consequently assigned to C_{60} crystals. Although the films thickness is in the range of $\sim 100\text{nm}$ and the microcrystals are in the range of μm , no pin holes were detected on the surface of the films. In Fig. 3, the photovoltaic properties devices made from blends of PPV with the three

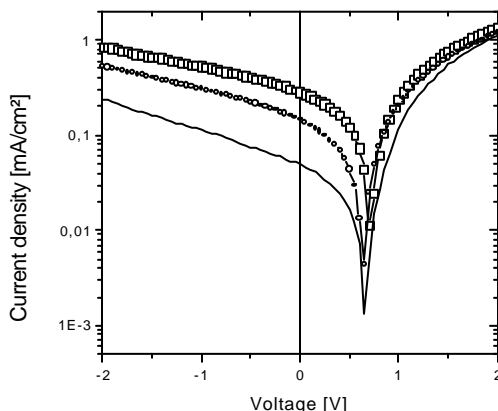


Figure 3: Current – Voltage curves of MDMO-PPV photovoltaic devices containing different fullerene derivatives: PCBM monoadduct (open squares), PCBM multiadduct (solid line) and C_{60} (small open circles).

different fullerenes are recorded under illumination with 6 mW/cm² white light from a luminescence tube. The highest short-circuit current is observed when PCBM monoadduct is used as electron acceptor ($|I_{sc}| = 280 \mu\text{A}/\text{cm}^2$). PCBM multiadduct devices show the lowest short circuit current ($|I_{sc}| = 50 \mu\text{A}/\text{cm}^2$) while devices using C₆₀ as electron acceptor yield a short circuit current in between ($|I_{sc}| = 145 \mu\text{A}/\text{cm}^2$). As a second polymer P3OT was investigated for the interplay between the quality of the interpenetrating network with the photovoltaic efficiency. Figure 4 illustrates an AFM comparison of P3OT/C₆₀ and P3OT/PCBM composite films. P3OT/C₆₀ composite films show rather homogeneous, but rough films in the sub- μm scale. In contrast, the P3OT/PCBM blend films show strong phase separation on a horizontal scale of several μm . Evidence of pinholes with depths of $\sim 30 \text{ nm}$ is also seen in the P3OT/PCBM films. The I/V characteristics for photovoltaic devices produced from these two composites are shown in Figure 5 together with the I/V behavior of a MDMO-PPV/PCBM device as reference. Comparable values were observed for MDMO-PPV/PCBM and P3OT/C₆₀ flexible large area plastic solar cells (IPCE $\sim 20\%$ under an argon laser at 488 nm with 10 mW/cm², $I_{sc} \sim 800 \mu\text{A}/\text{cm}^2$).

The I_{sc} of the P3OT/PCBM devices is almost a factor of two smaller than the devices mentioned above. The typical V_{oc} values for our devices on flexible ITO covered polyester substrates are around 700 mV, which can not be explained by a simple metal-insulator-metal (MIM) tunnel diode picture. The work function difference of the two electrodes ($\text{Al} = 4.3 \text{ eV}$; $\text{ITO} = 4.7 \text{ eV}$) is expected to yield $V_{oc} \sim 0.4$ in the MIM picture [9]. Furthermore, for different work functions of the anode material (Ca, Au), comparable V_{oc} values were observed in our devices. The formation of space charge layers at the electrode/polymer interface may lead to local potentials influencing the open circuit potential. Capacitance measurements are in progress to investigate the nature of the inorganic/organic interfaces in interpenetrating network solar cells.

The overall energy conversion efficiency, η_e , for the P3OT/C₆₀ as well as for the MDMO-PPV/PCBM flexible plastic solar cells was calculated to be approximately 1.5% under monochromatic illumination with (488 nm).

The photovoltaic external quantum efficiency (charge carrier per incident photon) or the spectrally resolved incident photon to converted electron efficiency IPCE (η_c) is

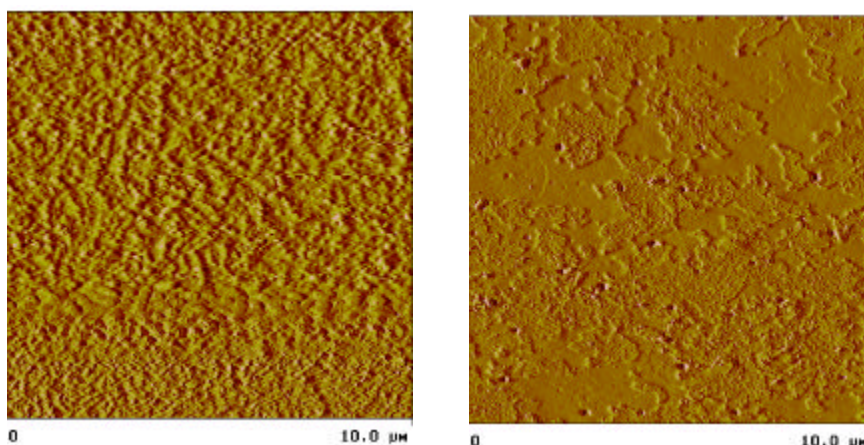


Figure 4: AFM comparison of P3OT/C₆₀ (1:1 weight ratio, left picture) and P3OT/PCBM monoadduct (1:2 weight ratio, right picture) composite films.

calculated from the spectrally resolved short-circuit current,

$$\eta_c[\%]= 1240/\lambda[\text{nm}] *I_{sc}[\mu\text{A}/\text{cm}^2]/I_{inc}[\text{W}/\text{m}^2]$$

where I_{inc} is the intensity of the incident light. The maximum value of the electron to photon conversion efficiency of an MDMO-PPV/PCBM solar cell is found to be app. 20% at 488 nm, which is comparable to the earlier reports [6, 10].

CONCLUSION

Photovoltaic devices fabricated from various blends of MDMO-PPV or P3OT as donors and [60]fullerenes or methanofullerenes (PCBM) as acceptors, show open circuit voltages up to 700 mV as well as short circuit currents up to 1 mA/cm². Partial crystallization, demixing and /or phase separation of the interpenetrating network on the film surface was observed by AFM spectroscopy for some donor / acceptor combinations. We have shown that low cost large area flexible plastic solar cells from P3OT sensitized with C₆₀ can be

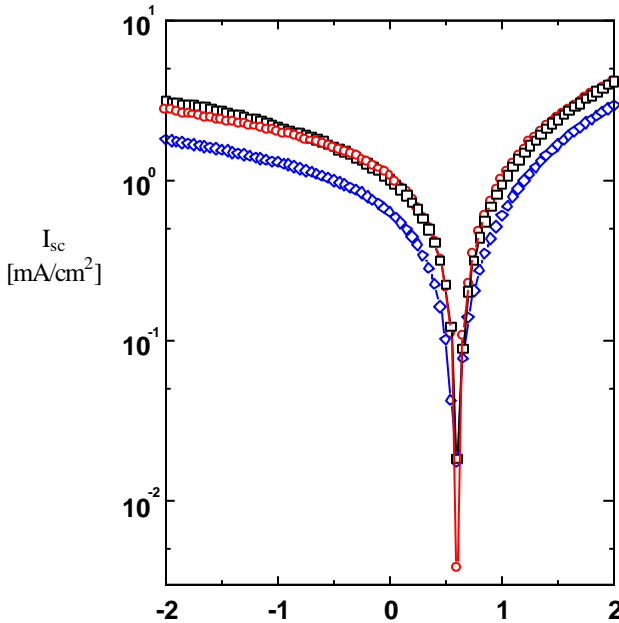


Figure 5: *I/V characteristics comparison between MDMO-PPV:PCBM (open squares), P3OT:C₆₀ (open circles) and P3OT : PCBM (open diamonds) devices under illumination with 20 mW/cm² with an argon laser of flexible large area plastic solar cells.*

fabricated, which are equally efficient and 'reliable' as the MDMO-PPV/PCBM large area flexible plastic solar cell. Under 10 mW/cm² monochromatic light at 488 nm the overall energy conversion efficiency, η_e , of a P3OT/C₆₀ flexible plastic solar cell presented here is calculated to be around 1.5 % with a FF = 0,3 and an IPCE of nearly 20%.

ACKNOWLEDGEMENT

This work is performed within the Christian Doppler Foundations dedicated laboratory on Plastic Solar Cells funded by the Austrian Ministry of Economic Affairs and Quantum Solar Energy Linz Ges. m. b. H. The work is further supported by the "Fonds zur Förderung der wissenschaftlichen Forschung" of Austria, the Magistrat Linz (Project No. P-12680-CHE) and the Netherlands Organization for Energy & Environment (NOVEM).

REFERENCES

- 1 N. S. Sariciftci, L. Smilowitz, A. J. Heeger and F. Wudl, *Science*, **258**, 1474 (1992).
- 2 N. S. Sariciftci, A. J. Heeger, *Handbook of Organic Conductive Molecules and Polymers*, ed: H. S. Nalwa (Wiley, New York, 1997), Vol. **1**, p. 437.
- 3 N. S. Sariciftci, D. Braun, C. Zhang, V. Srdanov, A. J. Heeger, G. Stucky and F. Wudl, *Appl. Phys. Lett.* **62**, 585 (1992); S. Morita, A.A. Zakhaidov and K. Yoshino, *Sol. State Commun.* **82**, 249 (1992).
- 4 G. Yu. J. Gao, J. C. Hummelen, F. Wudl, A. J. Heeger, *Science*, **270**, 1789 (1995).
- 5 M. Granström, K. Petritsch, A. C. Arias, A. Lux, M. R. Andersson & R. H. Friend, *J. Nature*, **395**, 257 (1998).
- 6 C. J. Brabec, F. Padinger, N. S. Sariciftci, J. C. Hummelen, *J. Appl. Phys.*, **85**, 6866 (1999).
- 7 N. S. Sariciftci, in *Handbook of Organic Conductive Molecules and Polymers*, ed: H. S. Nalwa, (Wiley, New York, 1997), Vol. **1**, p. 414.
- 8 J. C. Hummelen, B. W. Wright, J. Yao, C.L. Wilkins, F. Lepec and F. Wudl, *J. Org. Chem.* **60**, 532(1995).
- 9 L. R. Roman, M. R. Anderson, T. Yohannes, and O. Inganäs, *Adv. Mater.* **9** (15), 1164 (1997); K. Yoshino, K. Tada, M. Hirohata, H. Kajii, Y. Hironaka, N. Tada, Y. Kaneuchi, M. Yoshida, A. Fijii, M. Hamaguchi, H. Araki, T. Kawai, M. Ozaki, Y. Ohmri, M. Onoda and A. A. Zakhidov, *Synthetic. Met.* **84**, 477(1997).
- 10 C. J. Brabec, F. Padinger, J. C. Hummelen, R. A. J. Janssen, N. S. Sariciftci, *Synthetic Met.* **102**, 861(1999).